UCRL-91827 Rev. I
PREPRINT

THE RELATIONSHIP BETWEEN THE SHOCK SENSITIVITY AND THE SOLID PORE SIZES OF TATB POWDERS PRESSED TO VARIOUS DENSITIES (U)

R. Lee
G. Bloom
W. Von Holle
W. Weingart
L. Erickson
S. Sanders
C. Slettevold
R. McGuire

8th Detonation Symposium
Convention Center, Albuquerque, NM
July 15-19, 1985

July 31, 1985

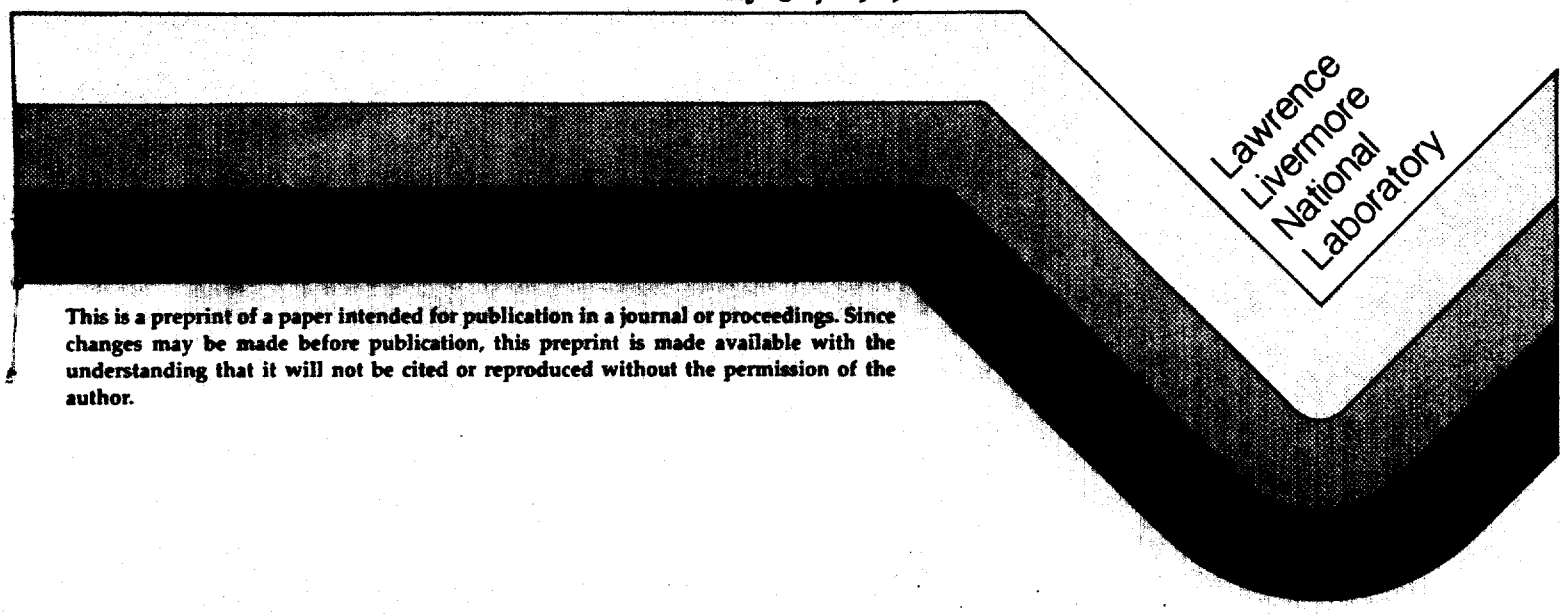

THE RELATIONSHIP BETWEEN THE SHOCK SENSITIVITY AND THE SOLID PORE SIZES OF TATB POWDERS PRESSED TO VARIOUS DENSITIES

R. Lee*, G. Bloom, W. Von Holle, R. Weingart, L. Erickson,
S. Sanders, C. Slettevold and R. McGuire

Lawrence Livermore National Laboratory
Livermore, California, 94550

ABSTRACT

Mercury intrusion porosimetry measurements have been made on samples pressed from three different types of TATB powders having quite different particle size distributions. The samples had densities ranging from 74-99% of theoretical maximum density. Results of the porosimetry measurements are compared with shock initiation thresholds measured on the same materials. The growth of reaction in sustained pressure experiments is also compared for two of the TATB types.

INTRODUCTION

Shock initiation of pressed secondary high explosives is due to concentration of energy at inhomogeneities in the material, leading to localized "hot spots" and subsequent reaction. The level of stimulus required to initiate a detonation is a strong function of the density to which the explosive is pressed. Internal voids have been proposed as one of the means by which the shock wave energy may be concentrated (1,2). Some of the proposed mechanisms include visco-plastic flow (3), adiabatic heating of trapped gas (4) and shocks generated by void collapse (5). In addition, it is well known that the shock initiation threshold depends on the particle size distribution of the powder from which the explosive specimens are pressed (6,7). In an earlier study (8) we observed particle size effects on the initiability of pressed TATB specimens. One of the major objectives of the work reported here was to study further the effect of high explosive microstructure on initiability.

Mercury intrusion porosimetry provides a method for directly investigating the voids in a pressed sample. We have made mercury intrusion porosimetry measurements on pressed samples of the high explosive TATB (triaminotrinitrobenzene) for three quite different particle size distributions. The samples investigated were pressed to densities that ranged from 74-99% of theoretical maximum density. We compare the results of the mercury intrusion measurements with shock initiation thresholds measured on the same material.

TATB SAMPLES

TATB is an extremely insensitive high explosive that can be prepared in a number of ways leading to quite different particle size distributions. Our baseline TATB material, which we call production grade (PG TATB), is produced in a two-step dry amination process, which leads to a product with an arithmetic mean particle size of 60 micrometres, as determined by wet sieving (8). The specific surface area of this material, determined by the BET method, is about 0.5 m^2/g (8).

A finer material can be prepared from the production grade TATB by wet grinding in a fluid-energy mill. We designate TATB produced by this method as ultrafine TATB (UF TATB). UF TATB has a mean arithmetic particle size of about 10 micrometres and a specific surface area of about 4.5 m^2/g, determined by the same procedures as for the production grade material (8).

TATB with a much finer particle size distribution has recently been synthesized

*Present address: Department of Physics, Cardwell Hall,
Kansas State University, Manhattan, KS.

(9,10). This material is prepared by crash-precipitation and is designated as CP TATB. Particle size distributions have been determined using a Coulter N4 particle sizer. The mean particle size of a CP TATB sample, determined by weight, was 0.22 micrometres. Specific surface area was measured on the same sample by the BET method using a Digisorb 2600 system, and we obtained a specific surface area of 17.1 m^2/g, although values for individual lots range from 7 to 30 m^2/g. Particle size was calculated from the surface area data, assuming spherical particles and a density of 1.9 g/cm^3, yielding a mean particle size of 0.18 micrometres in good agreement with the data from the Coulter instrument.

MERCURY INTRUSION POROSIMETRY

Mercury intrusion porosimetry is based on the law which describes the penetration of a liquid into a small orifice. For a non-wetting liquid and cylindrical pores, the minimum pore diameter, d, through which the liquid will flow at a pressure, P, is given by

$$D = (4\gamma/P)\cos(\theta), \qquad (1)$$

where γ is the surface tension of the liquid and θ is the contact angle between the liquid and the solid. Pore surface area is calculated from the PdV work required to force the mercury through the pores. The work dW that is needed to immerse an area dA of pore wall is given by

$$dW = \cos(\theta)dA = -PdV. \qquad (2)$$

The experimental technique consists of evacuation of a sample tube which contains the specimen to a pressure of 10^{-2} Torr and back-filling with mercury to 10 kPa to fill the sample tube completely and those pores which exceed 117 micrometres in diameter. The bulk density is determined at this point from the mass of the sample and the volume. Pressure is then applied at logarithmic intervals to a maximum of 200 MPa. The pore volume distribution is determined from the incremental volume change at each pressure increase, assuming that the pores are cylindrical. A skeletal density is determined at 200 MPa and compared with the theoretical maximum density of 1.937 g/cm^3.

SHOCK INITIATION THRESHOLD MEASUREMENTS

The shock stimulus required to initiate a detonation in the TATB samples was produced by the impact of a thin plastic flyer plate. The Mylar flyer plates were 0.25 mm thick and had diameters ranging from 1.00 to 25.4 mm. The flyer plates were accelerated by electrically exploding 25.4 x 25.4 x 0.051 mm aluminum foils with a capacitor bank system. The flyer plate material was driven by the explosion down a barrel of the desired diameter to impact the TATB specimen. A calibration curve of flyer plate velocity versus bank charging voltage was obtained using a Fabry-Perot laser velocity interferometer. The system which accelerated the flyer plates is described at length elsewhere (11).

The threshold velocity for shock initiation was determined using a delayed Robbins-Monro (DRM) procedure for selecting the bank charging voltages. The DRM protocol optimizes the information that can be obtained from the limited number of samples (usually 6-8) available for each threshold determination. The DRM procedure is also described in detail elsewhere in the literature (12). The shock initiation threshold data are summarized in Table 1.

INITIATION SPOT SIZE MEASUREMENTS

Figures 1 and 2 show the shock initiation threshold as a function of initiation spot size for four TATB forms. These are UF TATB; a UF TATB obtained from the AWRE, Aldermaston, England; CP TATB formulated at Livermore (designated CP-20), and a CP TATB designated CCP that was formulated at Los Alamos National Laboratory by Howard Cady. The data for both 1.4 and 1.6 g/cm^3 density show a sharp rise in threshold for the UF materials as the flyer diameter approaches 1 mm, while the data for the CP materials do not exhibit such a trend. There is also a reversal in sensitiveness of the UF and CP materials. The UF material is easier to initiate with the larger flyers, while the CP material is easier to initiate at the smaller flyer diameters. We also performed initiation threshold experiments at reduced temperatures (-54°C) and again observed a significant difference in the behavior of the CP and UF materials. We could not initiate the UF TATB at the lower temperature with 1.59 and 1.00-mm-diameter flyers, but the CP samples were initiated with only a modest increase in threshold velocity.

COMPARISON OF THRESHOLD AND POROSIMETRY RESULTS

Figure 3 shows the results of mercury intrusion porosimetry measurements made on pressed samples of CP, UF, and PG TATB. The difference between the curves for the CP and UF samples reflects the difference in two materials with different particle size distributions but the same density. The curve for the PG sample shows the effect of a higher density, as well as a different particle size distribution. Total intrusion volume and average pore diameter are listed for all the materials in Table II.

The porosimetry data correlate fairly well with the threshold velocity that a 0.25-mm-thick, 3.18-mm-diameter Mylar flyer plate must have to initiate a detonation in TATB.

TABLE I

Shock Initiation Threshold Data. Cady CP refers to CP material produced at LANL, CP-20 refers to CP material produced at LLNL, UF-AWRE is UF material obtained from AWRE, Aldermaston. The threshold data designated as "cold" were obtained from shots fired at -54°C. The threshold velocities marked "N" were shots which did not detonate at that impact velocity, so the true threshold velocity is somewhat higher.

EXPLOSIVE	THRESHOLD VELOCITY 25.4 MM FLYER (KM/S)	THRESHOLD VELOCITY 6.35 MM FLYER (KM/S)	THRESHOLD VELOCITY 3.18 MM FLYER (KM/S)	THRESHOLD VELOCITY 1.59 MM FLYER (KM/S)	THRESHOLD VELOCITY 1.0 MM FLYER (KM/S)
CADY CP (1.4 G/CC)	1.85	1.95	2.32	2.39	2.34
CADY CP (1.6 G/CC)	1.93	2.49	2.60	2.78	2.52
CADY CP (1.4 G/CC, COLD)	1.96			2.46	2.55
CADY CP (1.6 G/CC, COLD)				2.58	
CP-20 (1.4 G/CC)	1.99	2.12	2.18	2.36	2.37
CP-20 (1.4 G/CC)			2.18		
CP-20 (1.45 G/CC)			2.43		
CP-20 (1.50 G/CC)			2.52		
CP-20 (1.55 G/CC)			2.54		
CP-20 (1.6 G/CC)	2.29	2.63	2.84	2.72	3.20
CP-20 (1.60 G/CC)			2.79		
CP-20 (1.64 G/CC)			2.80		
CP-20 (1.70 G/CC)			2.99		
CP-20 (1.75 G/CC)			3.60 N		
CP-20 (1.80 G/CC)			3.60 N		
CP-20 (1.4 G/CC, COLD)	1.98			2.55	2.86
CP-20 (1.6 G/CC, COLD)	2.43			3.40	3.60 N
UF-AWRE (1.4 G/CC)	1.68	1.87	2.26	3.02	
UF-AWRE (1.6 G/CC)	2.01	2.07	2.35	3.07	
PRODUCTION (1.8 G/CC)	3.02				
ULTRAFINE (1.4 G/CC)	1.71	1.82	2.46	3.60 N	3.20 N
ULTRAFINE (1.6 G/CC)	1.91	1.95	2.35	3.60 N	3.60 N
ULTRAFINE (1.8 G/CC)	3.02				
ULTRAFINE (1.4 G/CC, COLD)	1.91			3.60 N	3.60 N
ULTRAFINE (1.6 G/CC, COLD)	2.07			3.60 N	3.60 N

TABLE II

Total pore volume and average pore diameter for some of the explosives tested.

EXPLOSIVE	DENSITY G/CC	TOTAL PORE VOLUME G/CC	AVERAGE PORE DIAMETER μm
CADY CP	1.40	0.1854	0.0339
CADY CP	1.60	0.0982	0.0194
CP-20	1.40	0.1761	0.0284
CP-20	1.40	0.1879	0.0431
CP-20	1.45	0.1665	0.0234
CP-20	1.50	0.1299	0.0184
CP-20	1.55	0.1162	0.0161
CP-20	1.60	0 0950	0.0175
CP-20	1.60	0.0933	0.0153
CP-20	1.65	0.0658	0.0117
CP-20	1.70	0.0455	0.0110
CP-20	1.75	0.0306	0.0118
CP-20	1.80	0.0205	0.0112
UF-AWRE	1.40	0.1880	0.0965
PRODUCTION	1.80	0.0454	0.0446
ULTRAFINE	1.40	0.1966	0.1192
ULTRAFINE	1.60	0.1092	0.0743
ULTRAFINE	1.80	0.0322	0.0128

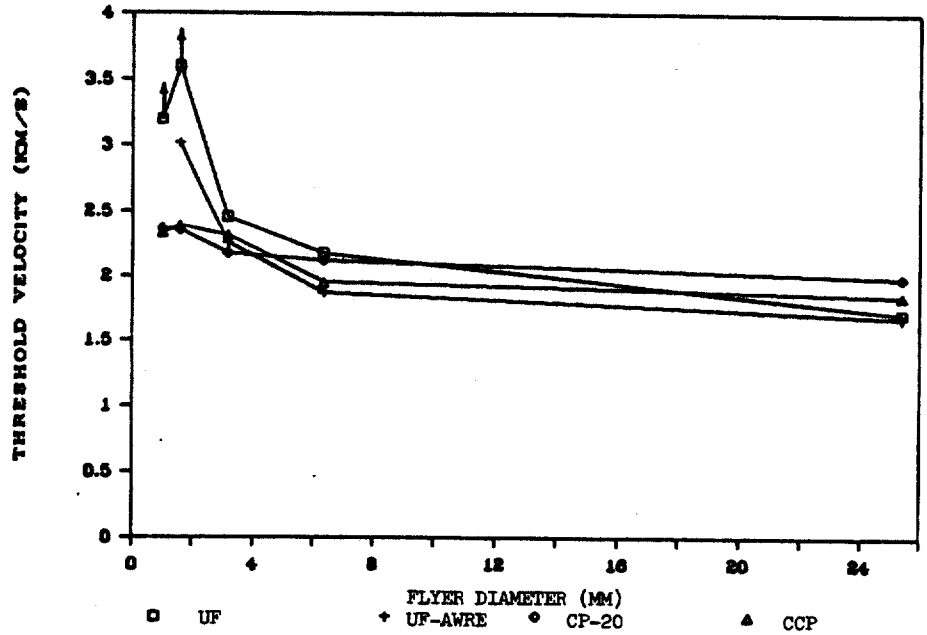

Fig. 1 - Threshold velocity for shock initiation, measured at ambient temperature. In the legend, UF, UF-AWRE, CP-20 and CCP refer respectively to ultrafine, British ultrafine, LLNL crash-precipitated and LANL crash-precipitated TATB. The vertical arrows denote failure to detonate at that velocity. All of the samples had density 1.4 g/cc

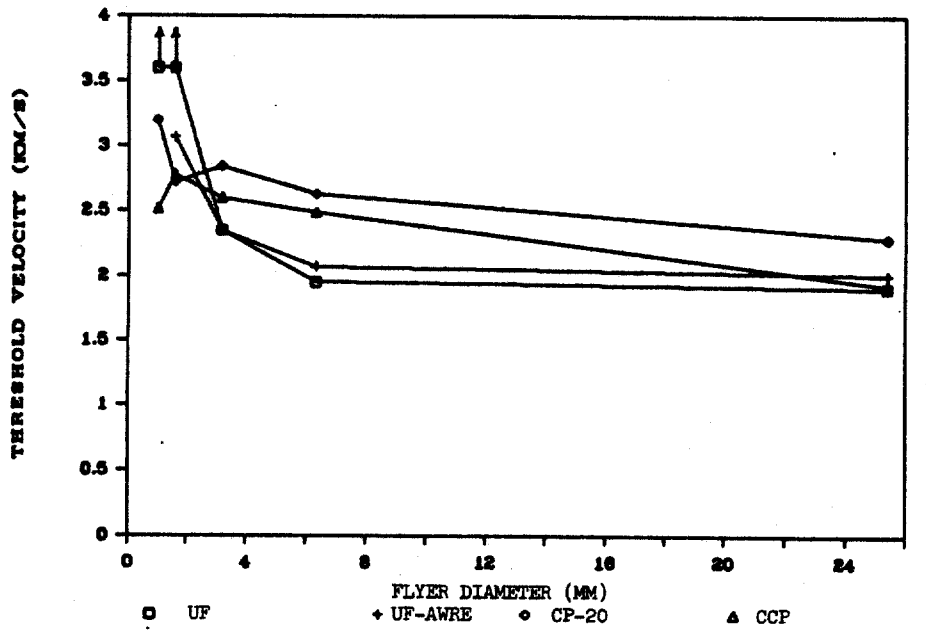

Fig. 2 - Threshold velocity for shock initiation, measured at ambient temperature. In the legend, UF, UF-AWRE, CP-20 and CCP refer respectively to ultrafine, British ultrafine, LLNL crash-precipitated and LANL crash-precipitated TATB. Vertical arrows denote failure to detonate at that velocity. All of the samples had density 1.6 g/cc

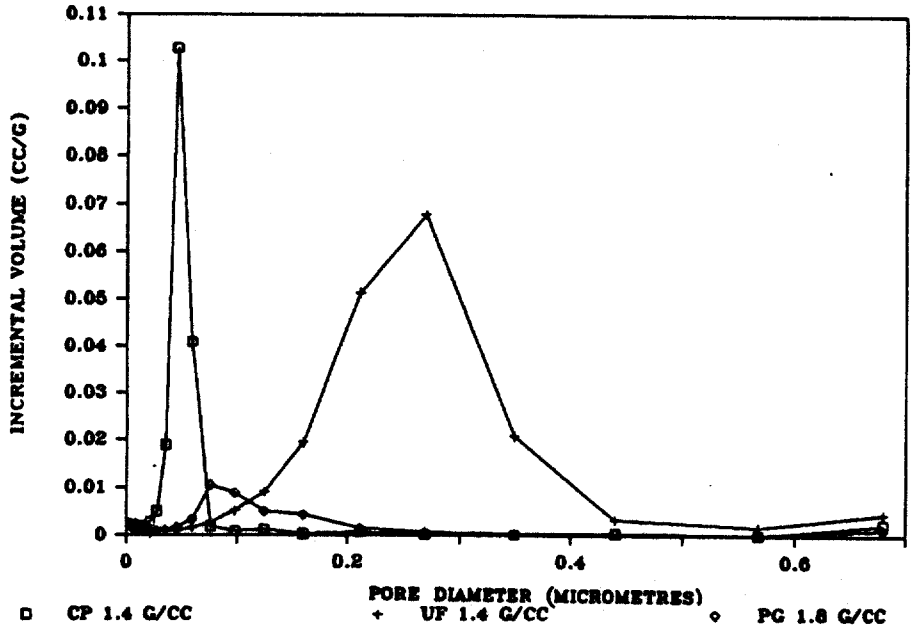

Fig. 3 - Incremental volume vs pore diameter for three TATB samples with different densities and particle size distributions. CP, UF and PG refer respectively to crash-precipitated, ultrafine and production-grade TATB.

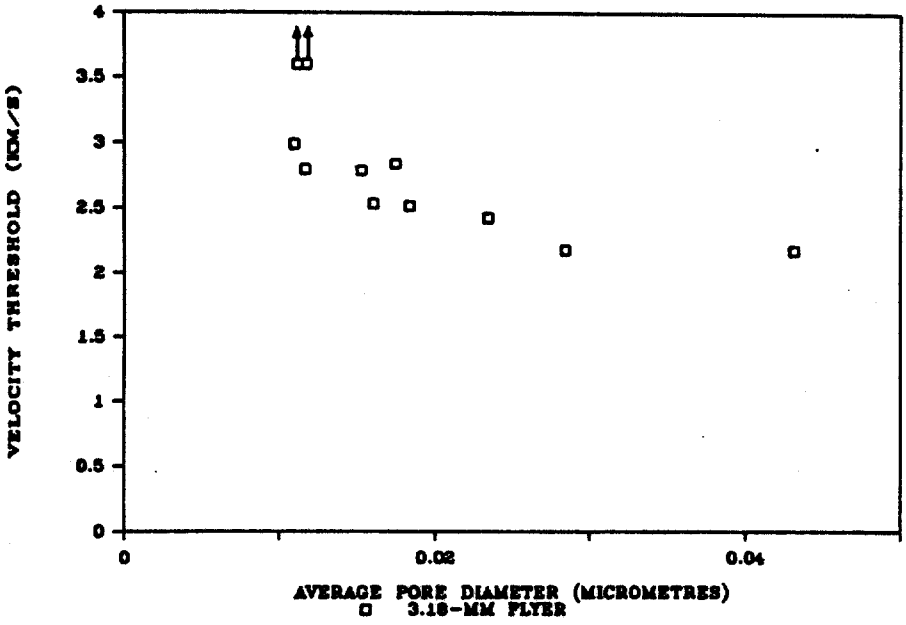

Fig. 4 - Velocity threshold vs pore diameter for crash-precipitated TATB pressed to various densities, 1.4 - 1.8 g/cc. Vertical arrows denote failure to detonate at that velocity.

In Fig. 4 we plot flyer velocity threshold for CP-20 versus average pore diameter as determined from 4V/A, where V is the total intrusion volume, A is the total void area and it is assumed that the voids are right circular cylinders.

In Fig. 5 we show the effect of pressing density on the void volume for samples of CP material. The figure clearly shows that pressing reduces the total pore volume and shifts the distribution of pore volumes toward smaller diameters. The effect of the change in density on velocity threshold is shown in Fig. 6. Density shows about the same degree of correlation with threshold velocity as does average pore diameter. In Fig. 7 we show the velocity threshold for 3.18-mm flyer impact as a function of average pore diameter for CP and UF TATB. At this flyer diameter, UF TATB has about the same threshold as CP, but has substantially greater average pore diameter. The dependence of the threshold on pore diameter is surprisingly weak, except for the smallest average pore diameters, where the curve rises steeply.

If a small-diameter flyer plate is used to initiate the TATB samples, we observe that pore diameter is not the only factor controlling the shock initiation threshold. Figure 8 shows the velocity threshold for 1.4- and 1.6-g/cc CP and UF TATB impacted by 1.0-, 6.35-, 3.18-, 1.59- and 1.00-mm-diameter flyers as a function of average pore diameter. The data points for pore diameters larger than 0.06 microns are for UF and UF-AWRE TATB and the data points for smaller pore diameters are for CP and CCP TATB. The velocity threshold for the CP material does not change much over the whole range of flyer diameters, while the threshold for the UF material increases drastically for flyer diameters less than 3 mm. This effect was also illustrated in Figs. 1 and 2. We attribute this difference in behavior between CP and UF material to the much-different particle size distributions. There are trivial chemical differences between the three types of TATB, especially between the CP and the two other materials, but the chemical differences do not lead to any marked thermochemical or performance differences. The remaining difference is in particle size and morphology. During shock compression, the intergranular forces will play a major role in determining the yield strength of the material and the way it fails when the yield strength is exceeded.

It must be recognized that pore size distributions calculated from mercury intrusion porosimetry data depend on the assumption that the sample is incompressible. In reality, porous samples may be crushed by the pressures in the sample cell, and the material from which the porous sample is made may be compressible. Figure 9 shows the total intrusion volume versus pressure for CP-20 TATB at 1.4-1.8 g/cc density. The solid line is the compression calculated from the bulk modulus of TATB. The bulk modulus was calculated from the sound speed measurements of Olinger and Hopson (13). At the higher pressures, the slope of the experimental curves approaches the slope of the calculated curve, suggesting that the apparent intrusion at these pressures is mostly due to compression of the TATB crystals. The curve for the 1.8 g/cc sample looks like virtually all of the apparent intrusion is due to compression of the sample. It is interesting to note the change in character of the curves between 1.6 and 1.7 g/cc density. This is the same density range where the initiation threshold increases sharply as shown in Fig. 6. Figure 10 shows the intrusion volume versus pressure for CP-20, PG and UF TATB at 1.8 g/cc density. At this density it appears that a good part of the intrusion is due to porosity for the UF and PG materials. One could correct for the sample compression by subtracting the calculated compressibility curve from the experimental curves and attributing the difference to intrusion of mercury into the pores.

102-MM-GUN EXPERIMENTS

The response of TATB to longer-duration pressure pulses has been studied using a 102-mm-gun facility that has been described elsewhere in the literature (14). Figure 11 shows stress gauge records from a PG TATB sample of density 1.80 g/cc that was impacted by a 12.5-mm-thick AD998 alumina flyer plate at 1.36 km/s, producing an 8 GPa pressure pulse. Figure 12 shows the stress-time records that were obtained when a UF TATB sample of 1.80 g/cc density was impacted by a 12.5 mm-thick AD998 alumina flyer plate at 1.36 km/s, producing a 10 GPa input pressure pulse. It is not possible to compare the run distances or times to detonation from these records, but it is clear from the record at the impact face that even at a higher input stress, the UF TATB reacts more slowly than the PG TATB. Also, the average shock velocity in the first 10 mm of run is considerably faster in the PG TATB. This behavior is consistent with earlier studies, where we observed that UF TATB is less sensitive than PG for sustained, lower pressure pulses, but for high pressures (>30 GPa) the UF material becomes more sensitive than the PG TATB.

SUMMARY AND CONCLUSIONS

We have measured shock initiation thresholds on TATB samples pressed from three different TATB powders which differ greatly in particle size distribution. The shock stimulus was produced by the impact of thin Mylar flyer plates accelerated by electrically-exploded metal foils. Flyer

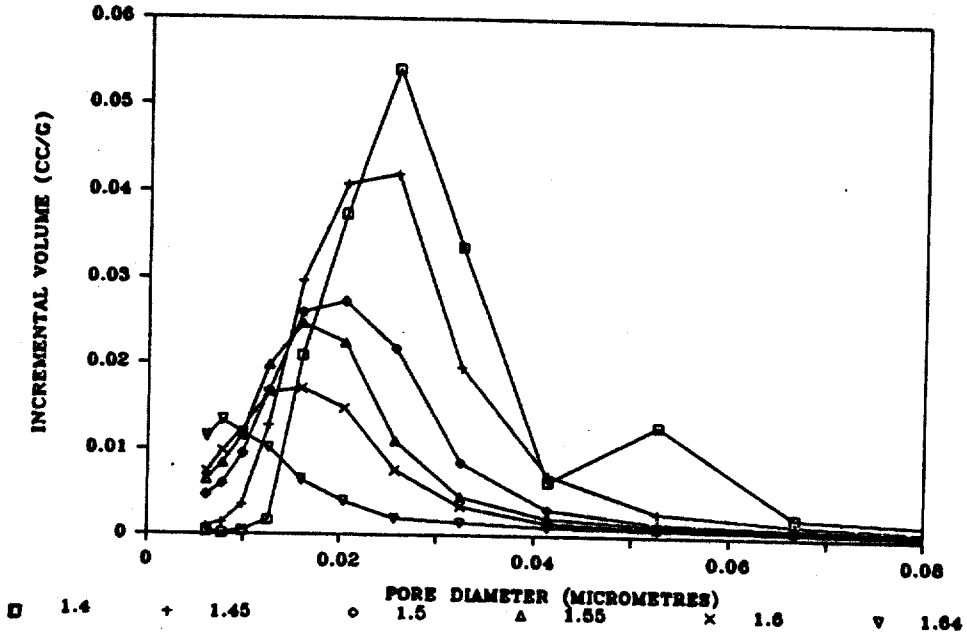

Fig. 5 - Incremental volume vs pore diameter for crash-precipitated TATB pressed to various densities, 1.4 - 1.6 g/cc. The numbers in the legend are the density in g/cc.

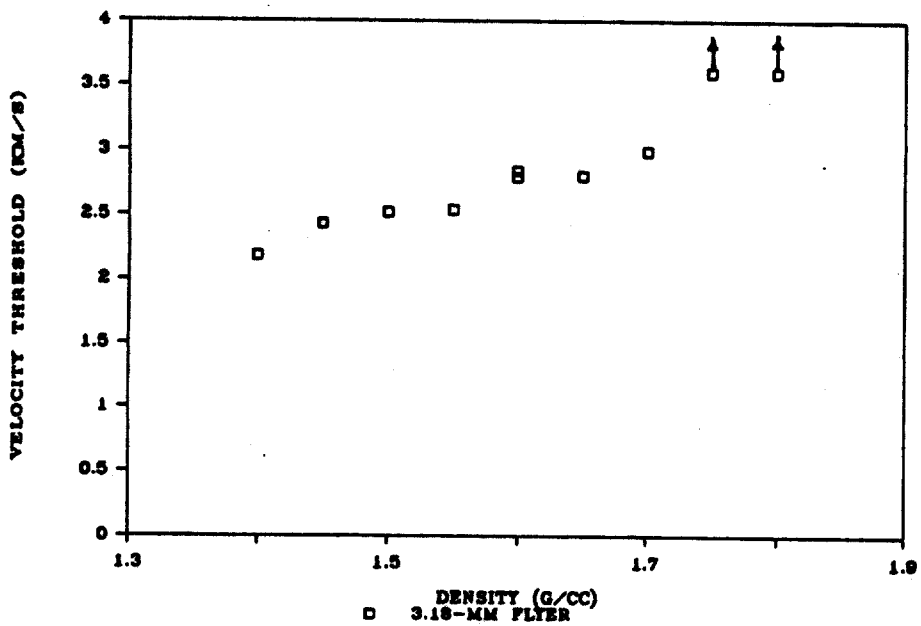

Fig. 6 - Threshold velocity vs density for shock initiation of crash precipitated TATB, CP-20. Vertical arrows denote failure to detonate at that velocity.

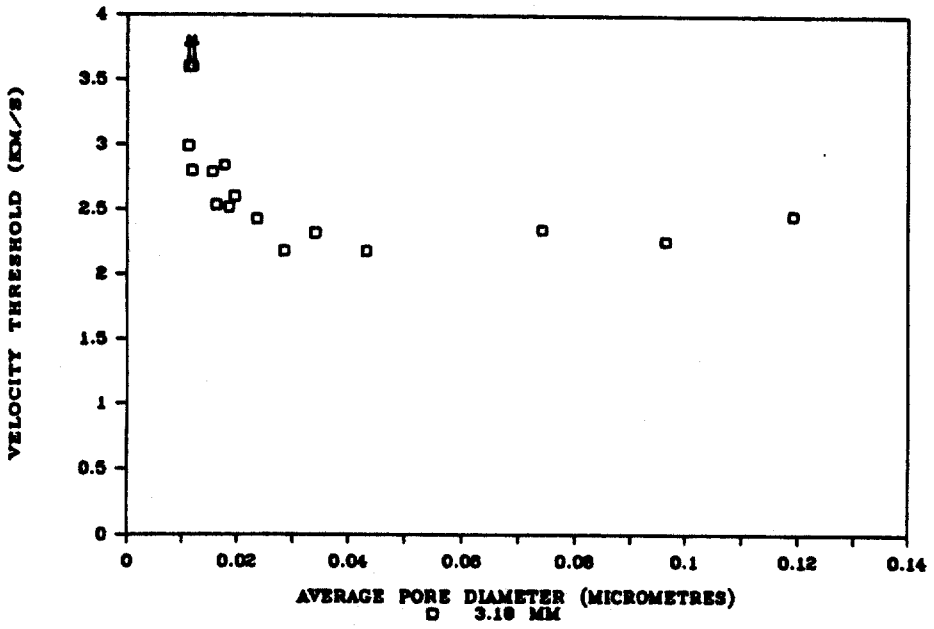

Fig. 7 - Velocity threshold versus pore diameter for ultrafine and crash-precipitated TATB at various densities, 1.4 - 1.8 g/cc. Vertical arrows denote failure to detonate at that velocity.

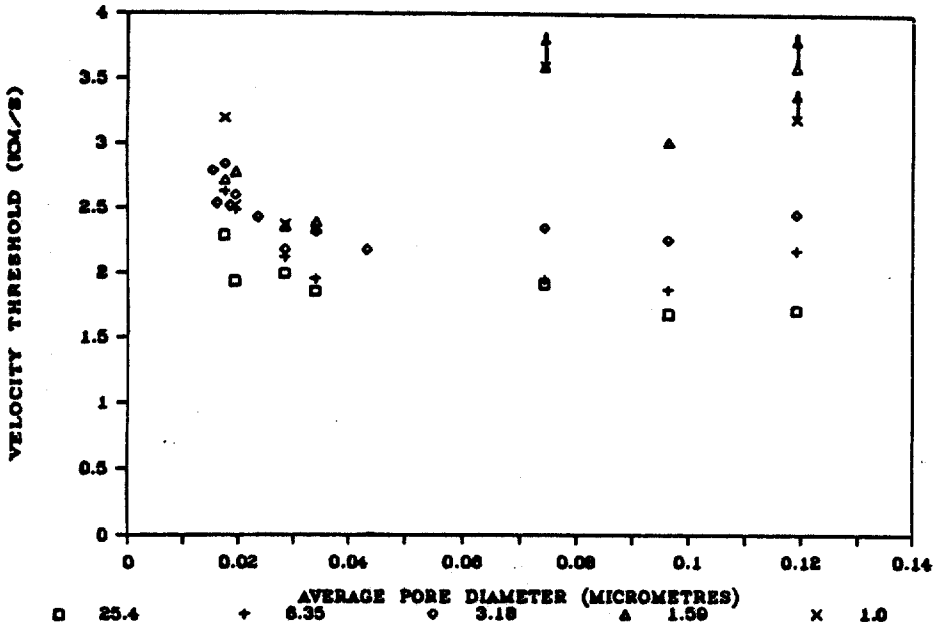

Fig. 8 - Velocity threshold vs pore diameter for ultrafine and crash-precipitated TATB for various flyer plate diameters, and various densities. The numbers in the legend are the flyer plate diameter in mm. Vertical arrows denote failure to detonate at that velocity.

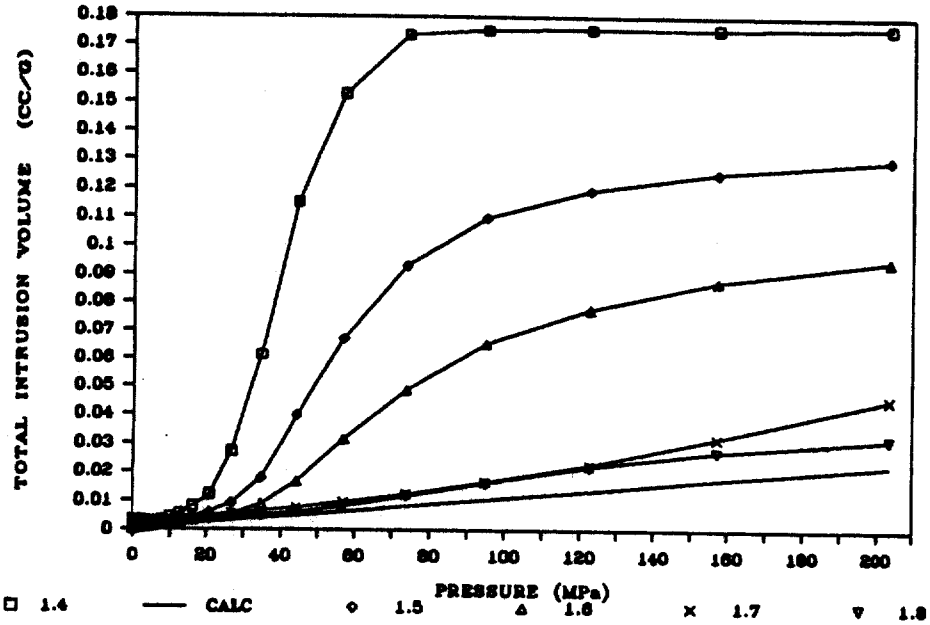

Fig. 9 - Intrusion volume vs pressure for crash-precipitated TATB, CP-20. The numbers in the legend are sample densities in g/cc. The solid line was calculated using a bulk modulus obtained from sound speed data.

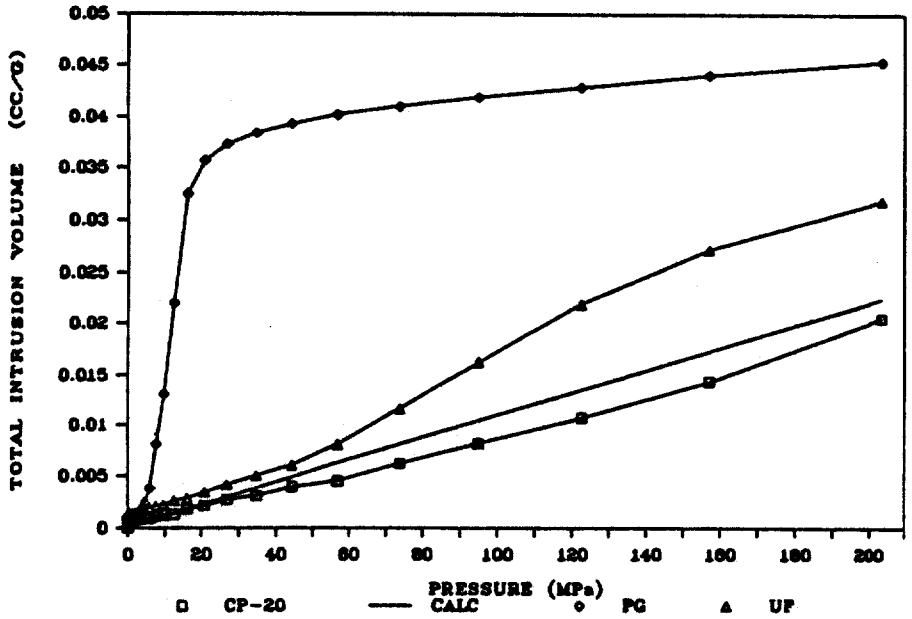

Fig. 10 - Intrusion volume vs pressure for crash-precipitated, ultrafine and production-grade TATB pressed to 1.8 g/cc density. The solid line was calculated using a bulk modulus obtained from sound speed data.

diameters ranged from 25.4 mm to 1.00 mm and flyer thickness was 0.25 mm.

The TATB powders were characterized by particle size determination and BET surface area measurements. The pressed samples were characterized by density measurements and mercury intrusion porosimetry.

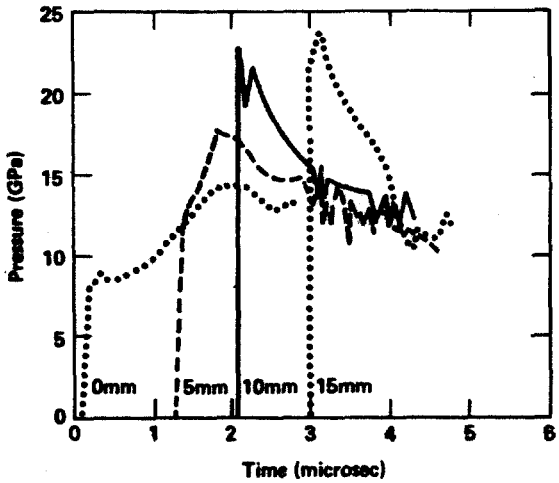

Fig. 11 - Manganin gauge records of pressure vs time recorded at 0, 5, 10, and 15 mm from the front surface of a production grade TATB sample impacted in a gun experiment to a pressure of 8 GPa. Sample density was 1.80 g/cc.

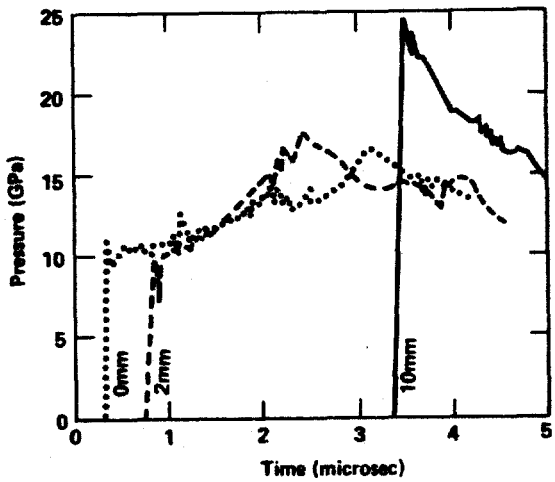

Fig. 12 - Manganin gauge records of pressure vs time recorded at 0, 2, and 10 mm from the front surface of an ultrafine TATB sample impacted in a gun experiment to a pressure of 9.8 GPa. Sample density was 1.80 g/cc

The shock initiation threshold correlated well with total intrusion volume and average void diameter for measurements made on samples of the same material which differed only in density. There was more scatter in the correlations observed when type of material as well as the density was varied, indicating that other variables besides void size distribution are important in the shock initiation process. For small-diameter flyer plates the difference between materials was particularly evident. For decreased flyer diameter the thresholds for the UF TATB rose dramatically, but did not increase appreciably for the CP TATB. Our results suggest that pore collapse may not be the dominant mechanism for producing reaction sites during shock initiation for densities below 1.65 g/cc, because large changes in the average pore diameter produced only modest changes in the shock initiation threshold.

ACKNOWLEDGMENTS

We gratefully acknowledge the generosity of H. Cady of Los Alamos National Laboratory for providing samples of his crash-precitipated material and to AWRE, Aldermaston, England, for sending us samples of ultrafine material, and thanks to Henry Chau for performing velocity calibration. Also, thanks to Robert Setchell of Sandia National Laboratory, Albuquerque for discussions on our use of mercury porosimetry.

*This work was performed under the auspices of the U.S. Department of Energy by Lawrence Livermore National Laboratory under contract No. W-7405-Eng-48.

DISCLAIMER

REFERENCES

1. A. W. Campbell, W. C. Davis, J. B. Ramsey, and J. R. Travis, Phys. Fluids 4, 511 (1961)

2. M. J. Frankel and D. J. Pastine, Proceedings of the Seventh Symposium (International) on Detonation, Office of Naval Research, NSWC MP 82-334 (1981) p. 523.

3. B. A. Khsainov, A. A. Borisov, B. S. Ermolaev, and A. I. Korotkov, Proceedings of the Seventh Symposium (International) on Detonation, Office of Naval Research, NSWC MP 82-334 (1981) p. 435.

4. Y. Partom, Proceedings of the Seventh Symposium (International) on Detonation, Office of Naval Research, NSWC MP 82-334 (1981) p. 507.

5. C. Mader, Phys. Fluids 8, 1811 (1965)

6. C. Scott, Proceedings of the Fifth Symposium (International) on Detonation, Office of Naval Research, ACR-184 (1970) p. 259

7. M. C. Chick, Proceedings of the Fourth Symposium (International) on Detonation, Office of Naval Research, ACR 126 (1965) p. 349

8. C. A. Honodel, J. R. Humphrey, R. C. Weingart, R. S. Lee, and P. Kramer, Proceedings of the Seventh Symposium (International) on Detonation, Office of Naval Research, NSWC MP 82-334 (1981) p. 425.

9. R. McGuire, LANL, Private communication.

10. H. Cady, LANL, Private communication.

11. R. C. Weingart, R. S. Lee, R. K. Jackson, and N. L. Parker, Proceedings of the Sixth Symposium (International) on Detonation, Office of Naval Research, ACR-2221 (1976) p. 653.

12. G. Bloom, H. Chau, R. Glaser, C. Honodel, R. S. Lee, and R. C. Weingart, Shock Waves in Condensed Matter-1983, North Holland, New York (1984) p. 535.

13. B. Olinger and J. W. Hopson, Actes du Symposium International sur le Comportement des Milieux denses sous Hautes Pressions Dynamiques, Ed. Commissariat a l'Energie Atomique Centre d'Etudes Nucleaires de Saclay, Paris, France, 27-31 Aout 1978. p. 9.

14. L. Erickson, Shock Waves in Condensed Matter-1981, Am. Inst. of Physics, New York (1982) p. 685.